

## GUIDANCE AND NAVIGATION FOR THE MARS PATHFINDER MISSION

Sam W. Thurman<sup>†</sup> and Vincent M. Pollmeier<sup>\*\*</sup>

Jet Propulsion Laboratory  
4800 Oak Grove Drive  
Pasadena, California, USA

The *Mars Pathfinder* Project is being developed by the U. S. National Aeronautics and Space Administration to demonstrate new technologies for landing on Mars, and to conduct focused, but significant, scientific observations. Scheduled for launch in December 1996 and arrival in July 1997, *Mars Pathfinder* is the second in the Discovery series of low-cost interplanetary missions. The principal challenge posed by this mission is the use of a ballistic atmospheric entry and descent scheme for landing. Delivery errors of no more than 25 to 50 km can be tolerated to achieve the desired entry corridor. Due to cost and schedule constraints, the navigational scheme must also be as simple as possible, taking advantage of existing capabilities. The guidance and navigation system developed to meet these requirements is described, along with the results of an analysis of the anticipated performance of that system.

### INTRODUCTION

The Mars *Pathfinder* Project has been initiated by the National Aeronautics and Space Administration (NASA) as the second mission in its Discovery program of small interplanetary missions, the first being the *Near-Earth Asteroid Rendezvous*. *Mars Pathfinder* will cost \$171 million to develop, excluding launch services and flight operations costs, over a three year period which began in November 1993. Its purpose is to demonstrate key technological capabilities for the delivery of payloads to the surface of Mars, and to conduct a set of focused, but significant, scientific observations of the Red Planet. The mission will be performed with a single flight system, launched by a *Delta // 7925* rocket equipped with a *PAM-D* upper stage. Launch will occur in December 1996 and arrival in July 1997. Upon landing, the spacecraft will initiate a 30 day surface operations period, including the deployment and operation of a small experimental rover. The rover will cost \$25 million to develop, and is being funded by NASA separately from the lander.

This paper presents an overview of the guidance and navigation system developed for *Mars Pathfinder*, and summarizes an analysis of its anticipated performance. The navigation problem poses a number of challenges, due to both the mission design and a desire to minimize the complexity of the spacecraft and its associated ground support systems. The most significant feature of the mission is the approach chosen for landing: the spacecraft will enter the Martian atmosphere directly from its interplanetary transfer trajectory, decelerate with the aid of a parachute and rocket braking, then reach the surface with a speed at impact of about 50 m/s, using an airbag system to cushion the vehicle from the shock. This scheme results in relatively stringent navigational accuracy requirements. In addition to the technical challenges to be met, the navigation-related requirements imposed on the spacecraft and the ground operations system must be kept to a minimum, due to the project's cost and schedule constraints.

---

<sup>†</sup> Member Technical Staff, Mission Design Section, Systems Division.

<sup>\*\*</sup> Acting Technical Manager, Navigation Systems Section, Systems Division.

## GUIDANCE AND NAVIGATION OVERVIEW

Like most interplanetary spacecraft, *Mars Pathfinder* will be guided toward its destination by propulsive maneuvers of short duration, separated by extended periods of ballistic flight. Navigation is accomplished through the reduction of radio tracking data to establish an estimate of the flight path, from which the maneuver computations are developed. A simplified illustration of this process is shown in Fig. 1. The process is an iterative one, in which the desired arrival conditions, specified as a set of target coordinates, are repeatedly compared with the best estimate of the actual target coordinates to determine the needed course corrections, which are implemented by command sequences. Flight operations will be conducted by a small team of 3 to 4 people, using a software system that largely resides on a single computer workstation, connected by a local network to other workstations within the project's ground data system.

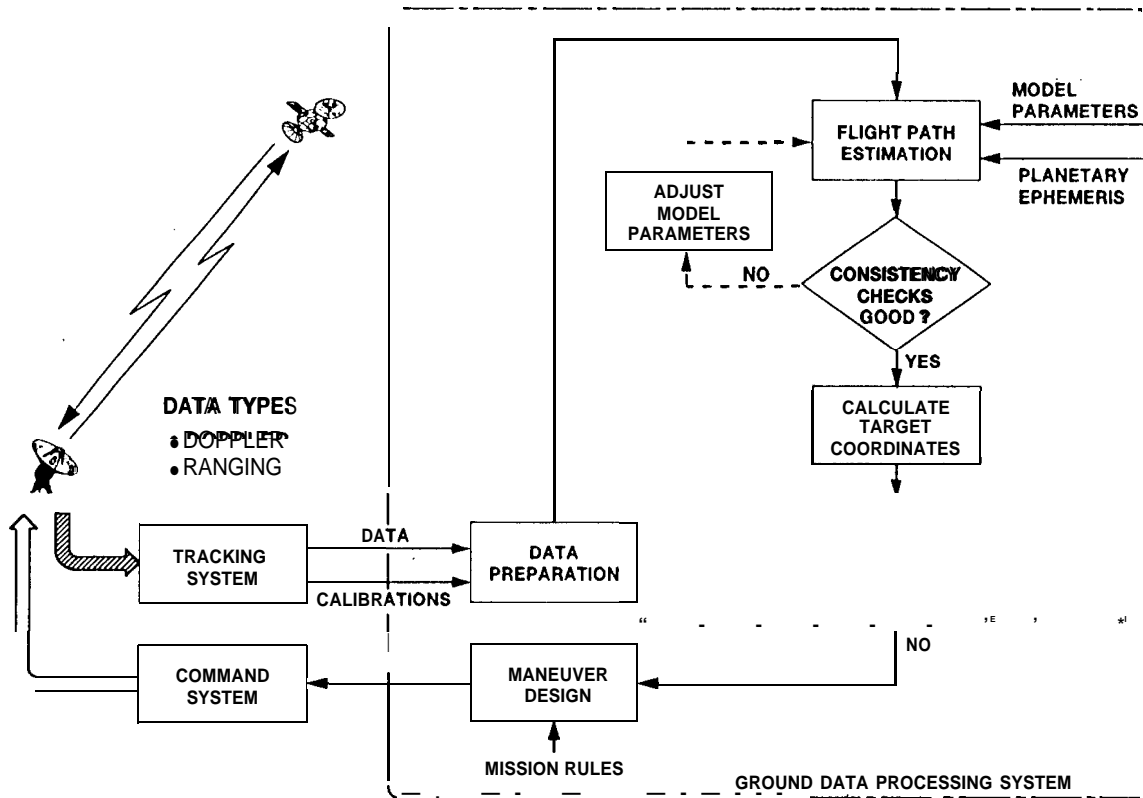


Figure 1: MARS PATHFINDER GUIDANCE AND NAVIGATION SYSTEM

The spacecraft is shown in its cruise configuration in Fig. 2. The upper disk-shaped portion is called the cruise stage, and houses the solar array, attitude sensors, a medium-gain radio antenna, and the propulsion subsystem. The cruise stage carries eight 4.45 N thrusters which will be used for both attitude control and course corrections, in order to minimize the complexity of the propulsion subsystem. The lander and rover are carried inside the **backshell** and **heatshield** in their stowed configurations. During cruise, the spacecraft will be spin-stabilized at a 2.0 rpm spin rate, with the solar array pointed at the Earth. As the spacecraft nears atmospheric entry, the cruise stage will be jettisoned once the entry vehicle has been placed in the proper entry attitude. A more detailed description of the mission is given by Cook and **McNamee**.<sup>1</sup>

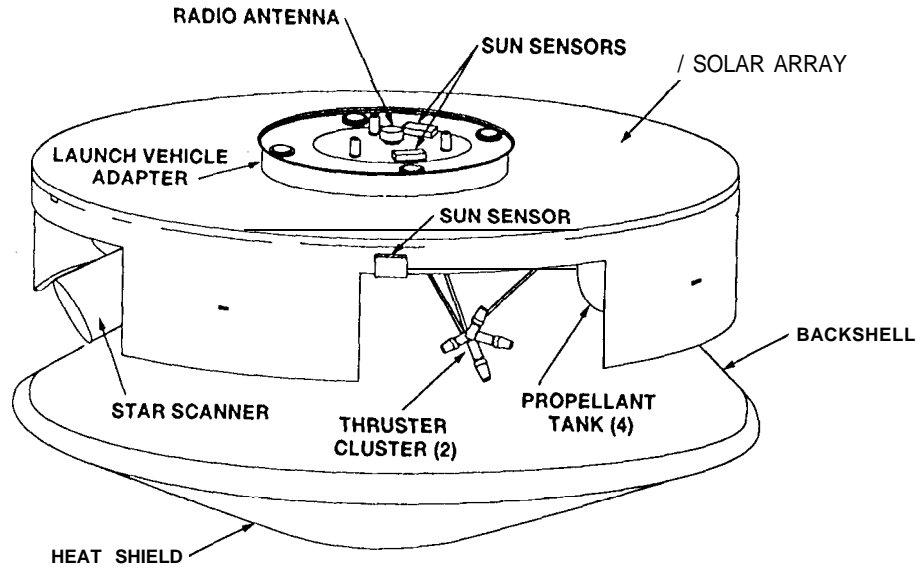


Figure 2: MARS PATHFINDER SPACECRAFT

### Navigational Requirements

The parameters defining the Mars approach trajectory must be controlled such that the spacecraft reaches the desired landing region with an acceptable error. An approximate, but useful illustration of the relationship between the atmospheric entry conditions and the trajectory parameters can be developed by treating the approach and entry trajectory as a hyperbola. The approach and entry geometry is shown in Fig. 3. The shape of the trajectory is established by the miss parameter,  $b$ , and the hyperbolic excess velocity,  $V_{\infty}$ . Specifically, the spacecraft's velocity at the entry interface,  $V_e$ , and flight path angle with respect to the local horizon,  $\gamma$ , are determined by  $b$  and  $V_{\infty}$ . Due to the dynamical properties of the approach trajectory, landing errors are determined principally by errors in the magnitude and spatial orientation of the miss vector,  $\mathbf{b}$ , which has magnitude  $b$ , and is oriented such that plane of the trajectory contains the target landing site at the nominal time of landing.<sup>2</sup>

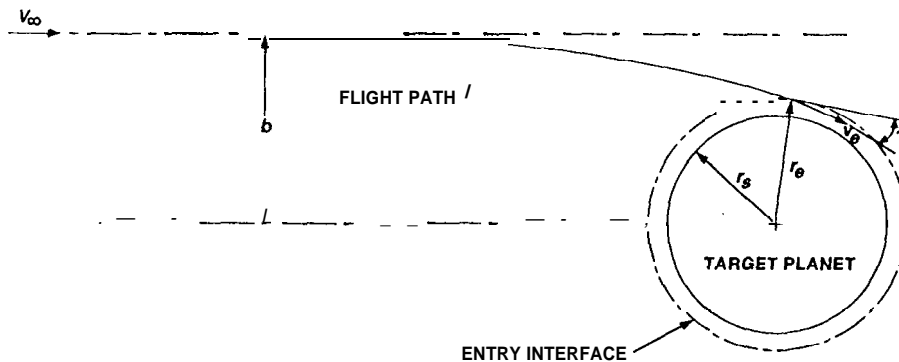


Figure 3: APPROACH TRAJECTORY AND ENTRY GEOMETRY

The value of  $V_{\infty}$  is established by the launch and arrival dates, The launch vehicle can support a 30 day launch opportunity period, beginning on 5 December 1996 and ending on 3 January 1997. The arrival date is fixed at 4 July 1997. The miss parameter,  $b$ , must be chosen such that the flight path angle,  $\gamma$ , matches some design value that leads to impact at the desired landing site. The relationship between  $\gamma$ ,  $b$ ,  $V_{\infty}$ , and the radius at entry,  $r_0$ , can be derived analytically from two-body mechanics:

$$\cos \gamma = \frac{b}{r_0 [1 + (2\mu)/(r_0 V_{\infty}^2)]^{1/2}} \quad (1)$$

In Eq. (1), the variable  $\mu$  is the product of the universal gravitational constant and the mass of the target body. For *Mars Pathfinder*, the design values of  $r_0$  and  $\gamma$  are 3522 km (125 km altitude) and -15.7 deg, respectively. The value of  $V_{\infty}$  ranges from 5.38 km/s to 5.51 km/s, depending upon the launch date. The largest value of  $b$  that will result in an impact trajectory for a given value of  $V_{\infty}$  can also be obtained from Eq. (1). This parameter, designated  $b^*$ , yields a radius at closest approach equal to  $r_0$ , the mean radius of Mars (about 3397 km). The desired expression is

$$b^* = r_0 [1 + (2\mu)/(r_0 V_{\infty}^2)]^{1/2} \quad (2)$$

The values of  $b$  and  $b^*$  obtained from Eqs. (1) and (2) are given in Table 1 for the first and last days of the launch opportunity period.

Table 1  
APPROACH TRAJECTORY PARAMETERS

Launch Date	$V_{\infty}$ , km/s	$b$ , km	$b^*$ , km
12/05/96	5.38	4600	4650
01/03/97	5.51	4550	4600

The relationship between landing errors and errors in targeting the design values of  $b$  and  $V_{\infty}$  has been analyzed with both analytical and numerical means, to establish the allowable navigation errors.<sup>2</sup> The planned Mars landing site is located at 15 deg N latitude, and 160 deg W longitude, in the *Amazonis Planitia* region. To achieve the desired delivery accuracy, with landing errors of no more than  $\pm 100$  km downrange and  $\pm 50$  km crossrange, the magnitude and orientation of the miss vector,  $b$ , must be controlled to within approximately  $\pm 25$  km and 0.8 deg (67 km in position relative to the target aim point), respectively. The requirement on  $b$  translates into an allowable error of  $\pm 1.0$  deg in  $\gamma$ . From Table 1, note that targeting errors in  $b$  of no more than about 50 km can be tolerated in order to avoid a skipout condition, regardless of the landing site.

### Guidance Strategy

The development of a guidance strategy involves determining how many maneuvers are needed, and the times at which they should be performed. The factors influencing these choices include the nominal trajectory, the injection accuracy of the launch vehicle, the delivery accuracy desired, and the accuracy of the flight path estimates used in the maneuver computations. For *Mars Pathfinder*, a series of four trajectory correction maneuvers (TCMs) has been established that provides sufficient control of the atmospheric entry conditions, and can be accomplished with relatively simple operational procedures. This maneuver schedule is given in Table 2, The time of each maneuver is specified relative to the elapsed time from launch (e.g., L +30 days) or the time prior to atmospheric entry at Mars (e.g., M -10 days).

Table 2  
NOMINAL PROPULSIVE MANEUVER SCHEDULE

<i>Maneuver</i>	<i>Time (days)</i>	<i>Description</i>
TCM-1	L + 30	remove injection bias, correct injection errors
TCM-2	L + 60	correct TCM-1 execution errors
TCM-3	M - 60	target spacecraft for Mars atmospheric entry
TCM-4	M - 10	correct TCM-3 execution errors

Note from Table 2 that the first maneuver, TCM-1, contains a deterministic component to remove a bias from the target coordinates supplied to the *Delta II* guidance system. The injection coordinates are intentionally biased away from the desired Mars atmospheric entry trajectory; the magnitude of the bias is chosen such that there is a 10<sup>-5</sup> probability that the *PAM-D* upper stage will be injected onto a Mars impact trajectory. This biasing must be employed to satisfy planetary quarantine requirements. The placement of the propulsive maneuvers along the nominal interplanetary transfer trajectory is shown in Fig. 4. This figure shows a view of the trajectory looking "down" from the north ecliptic pole. If the spacecraft is successfully launched on the first day of the launch period (5 December 1996), then the transit time to Mars will be 210 days; the tick marks along the trajectory denote 15 day time intervals. At the time of arrival, Mars is at a distance of approximately 1.27 astronomical units from the Earth.

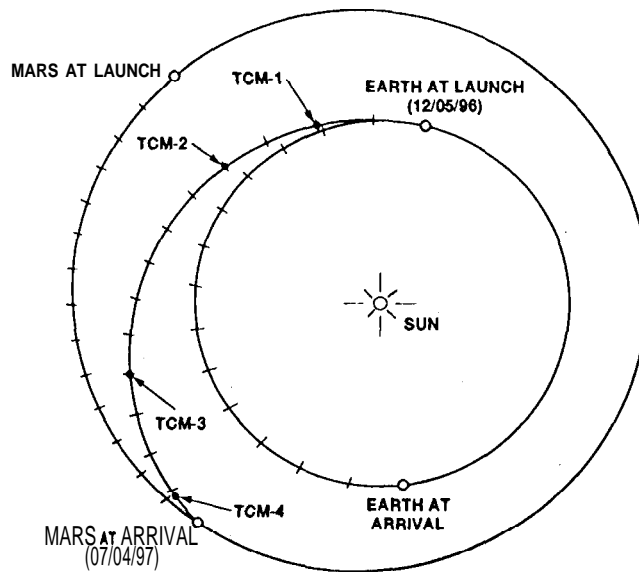


Figure 4: INTERPLANETARY TRANSFER TRAJECTORY

There are two possible maneuver implementation modes, the "vector" mode and the "turn-and-burn" mode. In vector mode (the nominal mode), two velocity changes are performed, one parallel to the spin axis and the other normal to the spin axis, such that their vector sum yields the desired velocity change. In this mode, the spacecraft maintains its nominal Earth-pointed attitude, permitting communication during the thruster firings. The axial component is performed by a continuous burn. The lateral component, normal

to the spin axis, is accomplished by pulsing selected thrusters over some fraction of a spin period. Due to its greater efficiency, the turn-and-burn mode can be used in the event of an extremely poor injection. In this mode, the spacecraft slews to orient its spin axis in the direction of the desired velocity change, executes a continuous burn, and then returns to its nominal attitude.

### Orbit Determination Strategy

Flight path estimation, or orbit determination, is a multi-faceted **process which** supports maneuver design, command sequence development, and tracking station pointing and frequency calculations. The measurements, or data types, which will be used are two-way Doppler and ranging data generated by ground stations of the Deep Space Network (DSN), operated for NASA by the Jet Propulsion Laboratory (JPL). These data are derived from a coherent radio link between the spacecraft and the receiving station.

The DSN Doppler system generates a precise cumulative count of the cycles of a Doppler tone during a tracking pass. In the two-way coherent mode of operation, the Doppler tone is derived from the difference between the transmitted and received carrier signals. A two-way Doppler measurement at time  $t_k$ , designated  $f_k$ , can be represented as

$$f_k = \frac{kf_o}{cT}(\rho_k - \rho_{k-1}) + b_f + f_t + f_i + f_{sp} + v, \quad (3)$$

In Eq. (3),  $p_k$  is the round-trip station-to-spacecraft range at time  $t_k$ ,  $f_o$  is the frequency of the transmitted carrier signal,  $k$  is the spacecraft transponder turnaround ratio,  $c$  is the speed of light in a vacuum, and  $T$  is the Doppler count interval, equal to  $t_k - t_{k-1}$ . The values of  $p$  are functions of the station location, the orientation of the Earth's polar axis, and the Earth-to-spacecraft distance. The term  $b_f$  represents a bias induced by the spacecraft's antenna radiation pattern, while the  $f$  terms represent tropospheric effects ( $f_t$ ), ionospheric effects ( $f_i$ ) and fluctuations in the interplanetary solar plasma ( $f_{sp}$ ), respectively. The variable  $v$ , represents the random noise component of Doppler measurement error. With proper calibration of the electronic and transmission media (troposphere, ionosphere, solar plasma) effects, Doppler data acquired in the X-band (7.2 to 8.4 GHz) have a typical accuracy of 0.01 to 0.02 mm/s over a 10 min count interval.

The DSN ranging system constructs an estimate of the round-trip light time to the spacecraft. This is accomplished by transmitting a range code with known period and frequency spectrum to the spacecraft, which coherently turns around the received code and retransmits it back to the ground station. The ranging system generates data points by repeatedly correlating the code received from the spacecraft with a model of the transmitted code. A two-way range measurement at time  $t_k$ , designated  $\tau_k$ , can be expressed as

$$\tau_k = \frac{\rho_k}{c} + b_R + b_T + \tau_t + \tau_i + \tau_{sp} + v_\tau \quad (4)$$

In Eq. (4),  $p_k$  and  $c$  have the same meaning as in Eq. (3),  $b_R$  represents a bias due to the ground station electronic delay, and  $b_T$  represents a similar bias due to the spacecraft transponder ranging channel delay. The remaining  $\tau$  terms represent transmission media effects, analogous to the  $f$  terms in the Doppler measurement model. The variable  $v_\tau$  represents the random noise component of the data. Under typical conditions, ranging accuracies of 1 to 2 m can be achieved over a 10 min observation time.

Doppler and ranging data will be collected by the DSN during routine tracking, telemetry, and command operations, according to the schedule given in Table 3. During critical periods such as the first few weeks after launch, trajectory correction maneuvers, and the approach to Mars, the spacecraft will be monitored closely. During relatively quiescent periods, less frequent coverage will be obtained. Tracking passes will be performed on a rotating basis between the DSN complexes near Goldstone, California in the U. S.,

Canberra, Australia, and Madrid, Spain. This rotating schedule reduces the impact of technical problems at a particular complex, and provides regular changes in the Earth-spacecraft observational geometry.

Table 3  
NOMINAL DSN DATA ACQUISITION SCHEDULE

<i>Phase</i>	<i>From</i>	<i>To</i>	<i>DSN Coverage</i>
Near-Earth	launch	<b>L+30</b> days	continuous
Transfer	<b>L+30</b> days	M-45 days	one 4 hr pass/week per complex
Mars Approach	M-45 days	arrival	continuous
TCMS	TCM-3 days	<b>TCM+3</b> days	one 8 hr pass/day; continuous for $\pm 12$ hr before and after TCM

The tracking data must be reduced using an estimation algorithm, or filter, to construct an estimate of the **spacecraft trajectory**. The filter **adjusts** Parameters in a mathematical model of the flight path and the measurement **error sources** in such a way that the data values predicted by the model are in the best possible agreement with the actual data and the statistical assumptions made. Seemingly small effects, such as solar radiation pressure and attitude control activity, must be modeled carefully. The navigational accuracy that can be obtained is heavily dependent upon the data reduction technique and the accuracy with which the spacecraft dynamics and the data can be modeled and calibrated. Until the development of high speed computer workstations, the sophistication of the filters employed operationally was limited by the cost and time needed for the computations. The onset of relatively cheap, but powerful computing platforms and graphic-oriented software tools now makes it possible to use sophisticated sequential filters routinely. For example, recent demonstrations conducted with the *Ulysses* and *Galileo* spacecraft, which focused on the use of sequential filtering techniques to model electronic and media calibration errors in high accuracy (2 to 5 m) ranging data, have shown that significant improvements (factors of 2 to 4) in navigational accuracy can be achieved relative to the techniques used previously in those missions.<sup>3,6</sup>

## PERFORMANCE ANALYSIS

The mission plan specifies that the spacecraft should be delivered to the target landing region with **99%** confidence. The statistics of the atmospheric entry targeting errors have been estimated through analytical means and Monte-Carlo simulation of the mission. Statistics of Av magnitude have also been estimated via Monte-Carlo simulation, in order to establish the guidance capability needed to correct for injection errors and subsequent maneuver execution errors. This section summarizes the key results of this analysis.

### Injection Accuracy

The injection aim point and the 99% probable dispersions in the Mars arrival B-plane<sup>1</sup> are shown in Fig. 5. The dispersion ellipse has semi-major and semi-minor axes of  $1.2 \times 10^6$  km and  $1.4 \times 10^5$  km, respectively. The 99% probable dispersion in the direction normal to the B-plane is  $1.0 \times 10^6$  km, or a time of arrival uncertainty of 2.1 days. The injection error statistics used in these computations are preliminary estimates developed by McDonnell-Douglas Aerospace Company, the manufacturer of the *Delta II* rocket.

<sup>1</sup> The B-plane is normal to the asymptote of the hyperbolic approach trajectory, and contains the miss vector, **b**, discussed earlier. Positional perturbations in the direction normal to the **B-plane** are closely related to perturbations in the time of flight to the target body along the approach trajectory, the difference between the two being a factor of **V**.

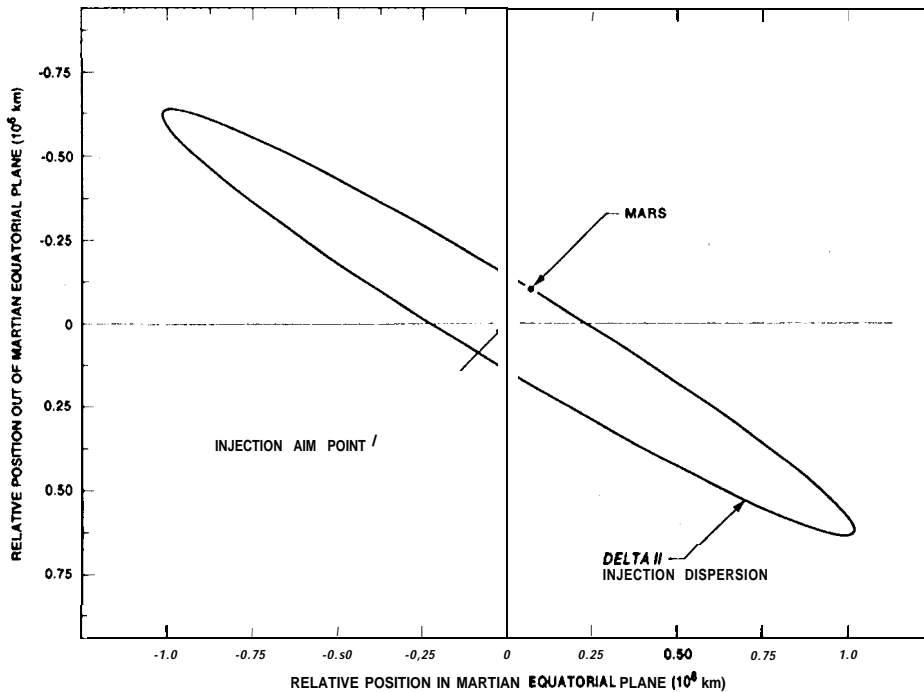


Figure 5: POST-INJECTION 99% *B*-PLANE TARGETING DISPERSIONS

### Delivery Accuracy

The 99% probable entry targeting dispersions in the Mars arrival *B*-plane are shown in Fig. 6. Results for three different cases are shown, assuming that navigation is performed with Doppler data only, ranging data only, or both Doppler and ranging data. Also shown is the ellipse defining the entry corridor that corresponds to the desired landing zone. In addition, two contours showing the maximum allowable deviations in the miss parameter,  $b$ , are shown. The skipout radius, defined by the parameter  $b^*$  from Table 1, corresponds to an entry angle of about  $-13.4$  deg relative to the local horizon. On the other extreme, if the entry flight path angle is steeper than  $-18$  deg, the deployment of the parachute would occur at too low an altitude to effect a landing. These statistics were derived from Monte-Carlo simulations of the navigation process; as such, they represent the aggregate targeting errors due to orbit determination error, maneuver execution error, and target body ephemeris error. The simulation procedure includes many systematic and statistical discrepancies between the "truth" models and the models used in the navigation filter, to reflect known simplifications in the filter model and to evaluate the effects of **mismodeling**.

The 99% dispersion in the direction normal to the *B*-plane, not shown in Fig. 6, is 100km(18s in time of flight) in the Doppler only case, and only 5 km (0.9 s in time of flight) in the cases involving ranging. From Fig. 6 it is evident that precise two-way ranging is a powerful technique, and has the added benefit that it is relatively simple from an operational standpoint. The desired landing accuracy is nearly achievable with ranging data alone, and can be met with both Doppler and ranging data. Doppler tracking, the simplest and most reliable radio metric technique, can also provide sufficient navigational accuracy to support a safe landing in the event of a failure in the spacecraft's ranging equipment. The assumptions and results of this analysis have been found to be qualitatively consistent with flight experience from *Mars Observer*, the most recent mission to employ the DSN's X-band tracking system.<sup>7</sup>

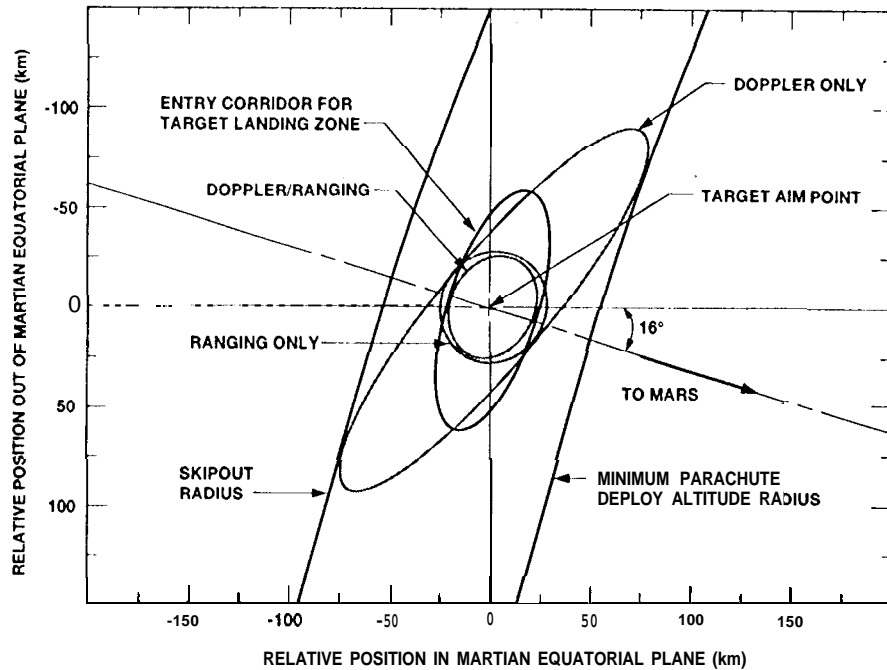


Figure 6: ATMOSPHERIC ENTRY 99% B-PLANE TARGETING DISPERSIONS

### AV Magnitude Statistics

The extent of the course corrections required for navigation are primarily a function of the injection accuracy of the launch vehicle and upper stage. To establish an appropriate propellant load for the spacecraft, estimates of the total  $\Delta v$  magnitude needed for guidance have been computed as part of the Monte-Carlo analysis described above. Due to the angled thruster configuration (see Fig. 2), the total velocity change delivered by the thrusters to perform a maneuver will be greater than the magnitude of the velocity change vector associated with that maneuver. The use of vector mode for maneuver implementation will result in additional propulsive inefficiency. The estimated  $\Delta v$  magnitude statistics are summarized in Table 4. Statistical parameters and confidence intervals were computed for the vector mode, a centingency scenario in which **TCM-1**, the largest maneuver, is performed in turn-and-burn mode (with all subsequent maneuvers performed in vector mode), and an idealized scenario in which all maneuvers are implemented with 100% efficiency.

Table 4  
STATISTICS OF GUIDANCE COURSE CORRECTIONS

Maneuver Mode	Total $\Delta v$ Magnitude (m/s)				
	Mean	Sigma	90%	95%	99%
vector	77	43	140	160	210
turn-and-burn	62	33	110	130	160
ideal	39	21	69	81	100

The statistics in Table 4 indicate that the amount of propellant needed to compensate for 99%, as opposed to 95%, of the probable injection errors is substantial. The data also show the penalties incurred in propulsive efficiency due to the thruster configuration and the use of vector mode. For this mission, it was decided to use a thruster configuration and maneuver implementation mode which minimized the complexity of the spacecraft design and the operational maneuver procedures, at the expense of additional propellant. Although it is relatively inefficient, vector mode is the preferred implementation mode, as radio contact can be maintained during maneuvers since no slewing of the spacecraft is required. In addition, the constant spacecraft attitude implicit in vector mode generally results in smaller execution errors. This is desirable, given the stringent accuracy requirements of the mission.

## SUMMARY

The *Mars Pathfinder* mission combines ambitious technical objectives with a fast-paced development schedule and a relatively modest budget. The guidance and navigation scheme created for the mission is designed to meet stringent accuracy requirements, while imposing as few requirements as possible on the spacecraft and the ground operations system. This system relies upon simple Doppler and ranging data acquired during routine tracking, telemetry, and command operations for navigation, and a guidance scheme in which a single propulsion system is used for both course corrections and attitude control. With the use of sequential data reduction techniques and low cost computer workstations, remarkable navigation accuracies can be achieved from a simple, yet reliable system,

## ACKNOWLEDGEMENT

The work described in this paper was performed at the Jet Propulsion Laboratory, California Institute of Technology, under contract with the National Aeronautics and Space Administration.

## REFERENCES

1. Cook, R. A., and J. B. McNamee, "Mission Design for the *Mars Environmental Survey*," Paper AAS 93-563, AAS/AIAA Astrodynamics Specialist Conference, Victoria, British Columbia, Canada, 16-19 August 1993.
2. Thurman, S. W., "Pathfinder Project Navigation Plan (Preliminary Version)," Report No. D-1 1349 (JPL internal document), Jet Propulsion Laboratory, Pasadena, California, December 1993.
3. McElrath, T. P., Tucker, B., Menon, P. R., and E. S. Higa, "*Ulysses* Navigation at Jupiter Encounter," Paper AIAA 92-4524, AIAA/AAS Astrodynamics Conference, Hilton Head, South Carolina, 10-12 August 1992.
4. McElrath, T. P., Thurman, S. W., and K. E. Criddle, "Navigation Demonstrations of Precision Ranging with the *Ulysses* Spacecraft," Paper AAS 93-687, AAS/AIAA Astrodynamics Specialist Conference, Victoria, British Columbia, Canada, 16-19 August 1993.
5. Pollmeier, V. M., Kallemeijn, P. H., and S. W. Thurman, "Application of High Precision Two-Way S-band Ranging to the Navigation of the *Galileo* Earth Encounters," *Advances in the Astronautical Sciences*, Vol. 84, Part 1, Univelt, Inc., San Diego, 1993, pp. 17-30.
6. Bhaskaran, S., Thurman, S. W., and V. M. Pollmeier, "Demonstration of a Precision Data Reduction Technique for Navigation of Interplanetary Spacecraft," Paper AAS 94-164, AAS/AIAA Spaceflight Mechanics Meeting, Cocoa Beach, Florida, 14-16 February 1994.
7. Cangahuala, L. A., Graat, E. J., Roth, D. C., Demcak, S. W., Esposito, P. B., and R. A. Mase, "*Mars Observer* Interplanetary Cruise Orbit Determination," Paper AAS 94-133, AAS/AIAA Spaceflight Mechanics Meeting, Cocoa Beach, Florida, 14-16 February 1994.